The EMBO Journal vol.15 no.10 pp.2393–2406, 1996

Cell cycle-controlled proteolysis of a flagellar motor protein that is asymmetrically distributed in the *Caulobacter* predivisional cell

Urs Jenal[1] and Lucy Shapiro[2]

Department of Developmental Biology, Stanford University School of Medicine, Stanford, CA 94305-5427, USA

[1]Present address: Department of Microbiology, Biozentrum, University of Basel, Klingelbergstrasse 70, CH-4056 Basel, Switzerland

[2]Corresponding author

Flagellar biogenesis and release are developmental events tightly coupled to the cell cycle of *Caulobacter crescentus*. A single flagellum is assembled at the swarmer pole of the predivisional cell and is released later in the cell cycle. Here we show that the MS-ring monomer FliF, a central motor component that anchors the flagellum in the cell membrane, is synthesized only in the predivisional cell and is integrated into the membrane at the incipient swarmer cell pole, where it initiates flagellar assembly. FliF is proteolytically turned over during swarmer-to-stalked cell differentiation, coinciding with the loss of the flagellum, suggesting that its degradation is coupled to flagellar release. The membrane topology of FliF was determined and a region of the cytoplasmic C-terminal domain was shown to be required for the interaction with a component of the motor switch. The very C-terminal end of FliF contains a turnover determinant, required for the cell cycle-dependent degradation of the MS-ring. The cell cycle-dependent proteolysis of FliF and the targeting of FliF to the swarmer pole together contribute to the asymmetric localization of the MS-ring in the predivisional cell.

Keywords: *Caulobacter*/cell cycle/flagellum/FliF/proteolysis

Introduction

Bacterial flagella are rotating organelles that confer motility. The transmembrane portion of the flagellum is a complex motor that converts chemical energy into mechanical work (Larsen *et al.*, 1974; Manson *et al.*, 1977). The output from the motor is transmitted through a flexible hook to the filament which acts as a propeller (Silverman and Simon, 1974). There are at least 20 proteins that contribute to the structure of the flagellum and another 30 are used for its construction (Macnab, 1992). The correct assembly of this macromolecular structure requires complex regulatory and organizational events, some of which have been elucidated in the past decades (Shapiro, 1995).

The task of controlling assembly of the single polar flagellum in *Caulobacter crescentus* is complicated by inherent features of its asymmetric cell cycle. In this organism, cell division results in two morphologically and physiologically distinct progeny, a motile swarmer cell and a sessile stalked cell (shown schematically in Figure 1). While the progeny stalked cell acts as a stem cell, immediately reinitiating chromosome replication and cell division, these processes are delayed in the swarmer cell and are initiated only after it differentiates into a stalked cell later in the cell cycle. The flagellar assembly process is tightly coupled to the cell cycle, resulting in the construction of a single flagellum at the pole opposite the stalk in the predivisional cell. Later in the cell cycle, the flagellum is released during the swarmer-to-stalked cell transition. Thus, assembly and removal of this complex macromolecular structure are developmental events integral to the *C.crescentus* cell cycle.

These cell cycle events raise several fundamental questions. How are flagellar components controlled temporally and spatially during the cell cycle? How is the site of flagellar assembly selected and how are the motor components confined to that site? What mechanisms are involved in flagellar release and how does the cell cycle control this removal process? Recent genetic and molecular studies have at least partially answered the first question. Most genes coding for flagellar components are organized in a four-tiered regulatory cascade (Classes I–IV), in which the expression of a given class of genes requires the physical presence of all components encoded by the preceding class (Champer *et al.*, 1987; Newton *et al.*, 1989; Ohta *et al.*, 1991; Brun *et al.*, 1994). This results in a temporal succession of flagellar gene expression and protein assembly during the cell cycle. The onset of this genetic cascade is regulated by cell cycle checkpoints (Stephens and Shapiro, 1993; Stephens *et al.*, 1995), and it is thought that members of the highest gene class (Class I) communicate signals from the cell cycle to the flagellar hierarchy. Recently, a Class I component has been identified and named CtrA. It is a member of the response regulator superfamily, and has been shown to activate flagellar gene expression and to control the expression of other cell cycle events (Quon *et al.*, 1996). Transcriptional regulation also contributes to the compartmentalization of flagellar components in the predivisional cell. Some of the flagellar genes expressed late in the cell cycle (Classes III and IV) have been shown to be transcribed only from the chromosome present in the swarmer portion of the dividing cell, a process coordinated by the spatially controlled activation of another response regulator protein, FlbD (Gober *et al.*, 1991; Wingrove and Gober, 1994).

To address the remaining two questions, a key component of the flagellar motor, the MS-ring (Figure 1B), is investigated. The MS-ring anchors the motor in the cytoplasmic membrane, interacting with the C-ring switch apparatus on its cytoplasmic face (Francis *et al.*, 1992; Oosawa *et al.*, 1994) and with its axial extension, the rod, in the periplasm (Figure 1B). In *Salmonella typhimurium*, ~26 monomers of the FliF protein assemble into the MS-

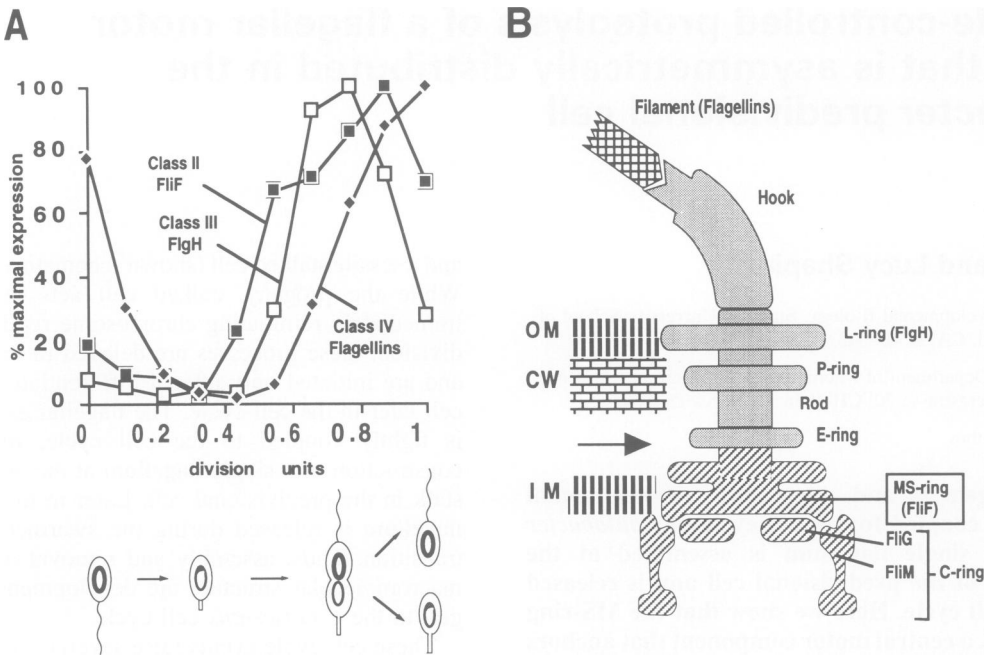

Fig. 1. Cell cycle-dependent expression of structural flagellar proteins. (**A**) Cell cycle expression of FliF (MS-ring), FlgH (L-ring) and flagellins (filament) analysed in synchronized cells of strain NA1000. Samples of cells were pulse labelled for 5 min with [^{35}S]methionine (5–10 μCi/ml) at the indicated stages of the cell cycle, harvested and used for immunoprecipitation with antisera specifically recognizing FliF, FlgH or flagellins, respectively. Expression was quantitated by phosphorimaging and plotted as a relative value of the highest expression point. The progression of cells through the cell cycle is indicated schematically. (**B**) Diagram of the *C.crescentus* flagellum. The flagellar structure is adapted from Driks *et al.* (1989), Stallmeyer *et al.* (1989b) and Trachtenberg and DeRosier (1992). The organization of the C-ring was adapted from that proposed for the *S.typhimurium* C-ring (Francis *et al.*, 1994; Zhao *et al.*, 1995). Flagellar structures composed of proteins encoded by Class II genes are marked with crossbars; structures composed of proteins encoded by Class III genes are stippled; the filament components encoded by Class IV genes are indicated by a squared pattern. Approximately 26 FliF protein subunits form the MS-ring structure which includes the M-ring, the S-ring and a short rod-like shaft (Jones *et al.*, 1990; Sosinsky *et al.*, 1992; Ueno *et al.*, 1992). The arrow indicates the position where the axial part of the flagellum is proposed to break off during flagellar release.

ring structure (Homma *et al.*, 1987; Jones *et al.*, 1990; Sosinsky *et al.*, 1992; Ueno *et al.*, 1992, 1994). Kubori *et al.* (1992) have shown that in enterics the MS-ring is formed in the absence of any other flagellar component, suggesting that flagellar assembly is initiated by insertion of the FliF protein into the membrane.

To understand how flagellar assembly is initiated in *C.crescentus*, it is necessary to define the mechanism used to target FliF to the pole opposite the stalk in the predivisional cell. The FliF protein could interact with a 'receptor' at the cell pole; alternatively, it could be retained at this site by another pole-specific feature either alone or in a complex with other flagellar components. The FliF protein is also likely to be a critical determinant in flagellar release during the swarmer-to-stalked cell differentiation. Flagella shed into the culture supernatant are ejected as filament–hook–rod complexes (Shapiro and Maizel, 1973; Stallmeyer *et al.*, 1989a), making the MS-ring–rod boundary a likely site for a proteolytic event leading to the loss of the axial components.

Here we show that the *C.crescentus* FliF protein is synthesized only in the predivisional cell where it is targeted to the swarmer pole. As a result of this, upon cell division, FliF ends up in the progeny swarmer cell but not in the progeny stalked cell. Later in the cell cycle, during the swarmer-to-stalked cell transition, FliF is proteolytically turned over, coincident with the loss of the flagellum. A small C-terminal cytoplasmic domain of FliF is required for its interaction with one of the C-ring proteins, FliG (Figure 1B), an interaction that is necessary for flagellar assembly and function. The C-terminus of FliF also contains a turnover determinant that marks the protein for degradation. We demonstrate that both the cell cycle-dependent turnover and targeting of FliF to the cell pole contribute to asymmetric localization of the MS-ring protein.

Results

The FliF protein is synthesized in the predivisional cell and proteolytically turned over later in the cell cycle during the swarmer-to-stalked cell transition

The FliF protein is the structural subunit of the flagellar MS-ring (Figure 1B). The formation of this ring is thought to be the first event in flagellar assembly (Kubori *et al.*, 1992). Consistent with this, the *C.crescentus fliF* gene is transcribed early in the predivisional cell (Ohta *et al.*, 1991). To investigate the expression, the steady state level and the polar segregation of the FliF protein during the *C.crescentus* cell cycle, we generated a polyclonal antibody that specifically recognizes FliF (see Materials and methods). The antibody recognized a single band corresponding to a protein of ~65 kDa (Figure 2A, lane 1), somewhat larger than the FliF protein size (56.8 kDa) deduced from the reported *fliF* nucleotide sequence (Ramakrishnan *et al.*, 1994). We propose, based on promoter and protein fusion experiments (data not shown),

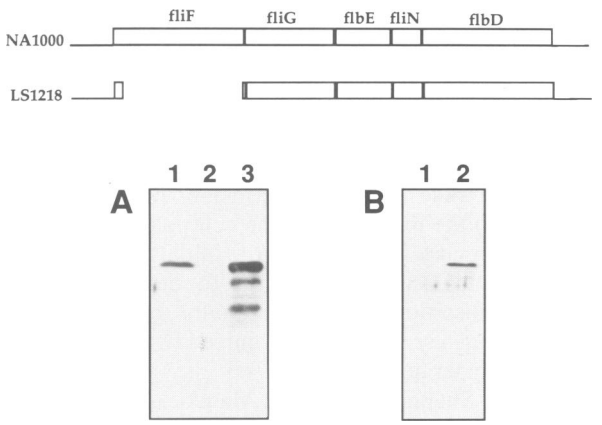

Fig. 2. Immunoblots of cell extracts with FliF antibody. The *fliF* operons in strains NA1000 and LS1218 are shown at the top. Anti-FliF antibody was raised in rabbits and tested for specific recognition of the *C.crescentus* FliF protein. (**A**) Crude extracts of strain NA1000 (wild-type, lane 1), LS1218 (NA1000Δ*fliF*, lane 2) and LS1534 (LS1218/pUJ62, lane 3) were separated on a 10% SDS–polyacrylamide gel, transferred to a polyvinylidine difluoride membrane (Immobilon-P, Millipore) and stained with anti-FliF antibody, as described in Materials and methods. The single band reacting with the serum corresponds to a protein of ~65 kDa in size. The protein is absent in the *fliF* null mutant strain LS1218, and is present in the same strain carrying the *fliF* wild-type gene on a plasmid (LS1534). In pUJ62, *fliF* is driven by its own promoter and an additional *lac* promoter, resulting in the overexpression of FliF protein. Two strong bands, corresponding to proteins of ~56 and 52 kDa in size, are regularly seen when FliF is overexpressed from a plasmid. They correspond most probably to degradation products of FliF. (**B**) The cytoplasmic fraction (lane 1) and the membrane fraction (lane 2) of strain NA1000 were isolated as described (Jenal *et al.*, 1994), and the same amounts of protein from both fractions were analysed as described in (A) for whole-cell extracts.

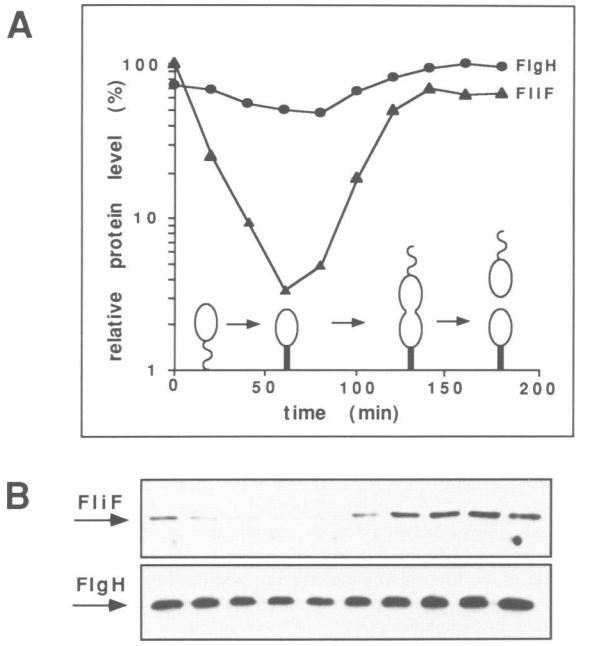

Fig. 3. Steady state levels of MS- and L-ring proteins throughout the cell cycle. (**A**) The graph shows FliF (MS-ring) and FlgH (L-ring) protein levels relative to their highest concentrations observed throughout the cell cycle. Progression of the cell cycle is indicated schematically. (**B**) The two panels show an immunoblot analysis with antibodies specifically recognizing FliF or FlgH protein (see Materials and methods; Jenal *et al.*, 1994). Total protein corresponding to the same culture volume of synchronized NA1000 cells was stained. The band intensities were quantitated with a densitometer, and the values obtained were used in the graphic representation shown in (A).

that the translational start site of *fliF* is 54 bp upstream of that reported previously (Ramakrishnan *et al.*, 1994). *fliF* initiating at the GTG (valine) codon (position 284 of the published sequence) would yield a slightly larger deduced molecular weight for the FliF protein (58.7 kDa). In contrast to the previously published start site, the new start site would not disrupt the proposed transmembrane spanning domain at the FliF N-terminus (see below). The 65 kDa protein was not detected in extracts of a *fliF* in-frame deletion mutant (Figure 2A, lane 2), but was detected in the Δ*fliF* strain with an extrachromosomal copy of the *fliF* gene (Figure 2A, lane 3). The additional lower molecular size bands observed in Figure 2A, lane 3 most probably correspond to degradation products of the FliF protein because they were observed consistently when the FliF protein was overexpressed. Together, these results demonstrate that the antibody specifically recognized the *C.crescentus* FliF protein. Separation of the cellular components into membrane and cytosolic fractions confirmed that FliF is an integral membrane protein (Figure 2B).

To determine when FliF is expressed during the cell cycle, samples of synchronized cultures were pulsed for 5 min with [^{35}S]methionine and labelled protein was immunoprecipitated with the FliF antibody (Figure 1A). FliF was not expressed in swarmer or nascent stalked cells but appeared at ~0.4 cell division units, shortly after the stalked cell initiated the division process. The time of appearance of FliF coincided with the reported activity of the *fliF* promoter (Ohta *et al.*, 1991), thus confirming the critical role of transcription in the temporal control of the expression of flagellar components. The time of appearance of the Class II FliF protein was also compared with the expression pattern of flagellar components encoded by Class III (FlgH) and Class IV (flagellins, filament) flagellar genes. FliF, FlgH and the flagellins appear in succession (Figure 1A), reflecting the temporal pattern of the flagellar transcriptional hierarchy (Brun *et al.*, 1994; Gober and Marques, 1995) and their order of assembly.

Later in the cell cycle, when the progeny swarmer cell differentiates into a stalked cell, the flagellum is shed. The released flagellar structures consist of a rod, hook and filament (Shapiro and Maizel, 1973; Stallmeyer *et al.*, 1989a). The fate of the motor components is unknown. Previously we showed that a component of the C-ring, FliM, is proteolytically turned over, coinciding with the loss of the flagellum (Jenal *et al.*, 1994). Immunoblots of cell extracts from synchronized cultures revealed that the FliF protein is also subject to proteolytic degradation during the swarmer-to-stalked cell differentiation, reaching its lowest concentration in the stalked cell (Figure 3). The protein then reappeared when the synthesis of FliF was turned on in the early predivisional cell (Figure 3). As discussed below, in nonsynchronized cells it takes a pulse time roughly equivalent to one cell cycle to degrade all the labelled FliF. This suggests that FliF is degraded specifically during the swarmer-to-stalked cell transition, and that the specific proteolysis of flagellar components at the base of the flagellum is either the cause or a consequence of flagellar release during this period of the

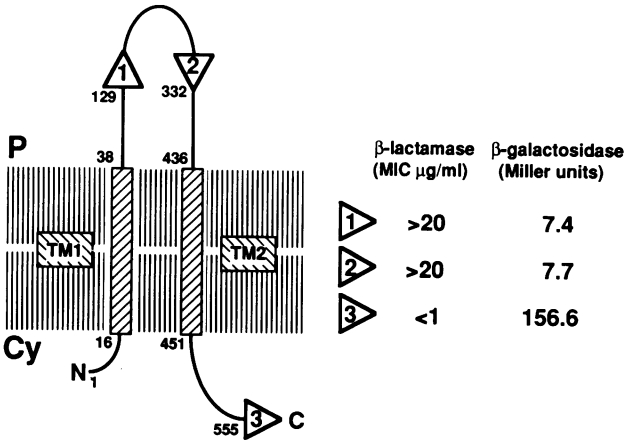

Fig. 4. Diagram of the proposed FliF membrane topology. The two potential membrane-spanning hydrophobic domains of FliF (TM1 and TM2) are shown embedded in the cytoplasmic membrane. The periplasmic (P) and cytoplasmic (Cy) regions are indicated. The start and end of the transmembrane domains and the fusion sites are indicated with the corresponding amino acid number of the FliF sequence. β-Lactamase and β-galactosidase fusion sites 1–3 are marked with triangles, and the enzymatic activities of the corresponding protein fusions in strains LS785–787 (β-galactosidase), LS1535, LS1702 and LS2252 (β-lactamase) are shown on the right. β-Galactosidase activity is shown in Miller units (Miller, 1972); β-lactamase activity was measured as the minimal inhibitory concentration (MIC) of ampicillin required to prevent growth of the strains carrying the corresponding constructs.

cell cycle. In contrast, the FlgH protein, the subunit that assembles into the L-ring in the outer membrane, was not turned over during the time of flagellar release (Figure 3), suggesting that there is a stable unassembled pool of FlgH protein present in the cell or, alternatively, that the L-ring structure becomes part of the new stalk.

Membrane topology of FliF

FliF is an integral membrane protein that contains two hydrophobic domains flanked by charged residues, one at its N-terminus (amino acids 16–38; TM1) and one close to the C-terminus (amino acids 436–451; TM2) (Figure 4; Ramakrishnan *et al.*, 1994). To determine the topology of FliF in the membrane, we generated protein fusions between FliF and a periplasmic protein, β-lactamase, or a cytoplasmic protein, β-galactosidase. The activity of these two enzymes is dependent on their proper cellular location. Thus, the topology of a membrane-spanning protein can be analysed by determining the enzymatic activity of the β-lactamase and β-galactosidase fusions (Manoil *et al.*, 1988; Manoil, 1990; Prinz and Beckwith, 1994). β-Galactosidase is only active in the cytoplasm, and β-lactamase is only active in the periplasm. As shown in Figure 4, fusions were generated at two different sites in the region between the transmembrane-spanning domains, and at the C-terminus (see Materials and methods). β-Galactosidase activity was detected with the C-terminal fusion (Figure 4, fusion 3) but not with the two internal fusions (Figure 4, fusions 1 and 2). In contrast, β-lactamase fusions conferred resistance to ampicillin only when fused between TM1 and TM2 (Figure 4, fusions 1 and 2) but not when fused at the C-terminus (Figure 4, fusion 3). We conclude that most of the FliF protein (amino acids 39–435) is located in the periplasm, while the N- and C-terminal portions of FliF are exposed to the cytoplasm.

The FliF protein is targeted to the swarmer pole of the predivisional cell, where it initiates flagellar assembly. There are two possible routes for FliF to reach the pole: it is either randomly inserted into the membrane and then reaches the pole by lateral diffusion, or it is inserted directly into the membrane at the cell pole by a localized export machinery. In each case, the initial step is insertion into the cytoplasmic membrane. To determine if FliF membrane insertion is dependent on the general secretory pathway (Pugsley, 1993), we examined two independently isolated temperature-sensitive (ts) *secA* mutant strains (Kang and Shapiro, 1994; J.R.Maddock, C.M.Stephens and L.Shapiro, unpublished data) for the insertion of FliF into the membrane fraction. The relative amount of FliF protein inserted into the membrane was determined by the immunoprecipitation of [^{35}S]methionine-labelled protein after shift to the nonpermissive temperature and subsequent separation of the membrane and cytosolic fractions. FliF incorporation into the membrane was found to be unaffected in strains carrying either mutant allele (data not shown). In contrast to this, β-lactamase processing has been shown to be reduced drastically in both *secA* mutant strains upon shift to the nonpermissive temperature (Kang and Shapiro, 1994; C.N.Stephens and L.Shapiro, unpublished data). It appears, therefore, that membrane insertion of the FliF protein in *C.crescentus* is not dependent on the general secretory pathway.

The C-terminus of FliF is required for flagellar assembly and cell cycle-dependent proteolysis

The FliF protein carries information that (i) targets it to the swarmer pole of the predivisional cell, (ii) contributes to its interaction with other proteins that are assembled into a functional flagellum, and (iii) dictates its proteolytic removal later in the cell cycle, coincident with release of the flagellar structure. To define the parts of the FliF protein that are required for each of these functions, we generated deletions in its cytoplasmic C-terminal domain and analysed the phenotype of the resulting mutants. Figure 5A shows an amino acid sequence comparison of the *C.crescentus* (Ccr) and *S.typhimurium* (Sty) FliF C-termini (Jones *et al.*, 1989; Ramakrishnan *et al.*, 1994). The location of the transmembrane domain (TM2) is indicated by a box. Five different in-frame deletion alleles (Δ*1*–Δ*5*) were constructed in the domain immediately following TM2: In Δ*1*, a stretch of 22 internal amino acids unique to the *C.crescentus* sequence was deleted; in Δ*2*–Δ*5*, decreasing amounts of the C-terminus were deleted (72, 57, 41 and 26 amino acids; Figure 5A). The five deletion alleles were cloned into the broad host-range plasmid pGL10, yielding pUJ99–pUJ103 (Table I). These plasmids were introduced into both *C.crescentus* wild type (NA1000) and NA1000Δ*fliF* (LS1218; see Materials and methods) and all resulting strains were tested for motility. As shown in Figure 5B, only the Δ*1* allele was able to complement the motility defect of the *fliF* null mutant strain LS1218. Strains carrying the alleles Δ*2*–Δ*5* on a plasmid were only motile in the presence of a chromosomal wild-type copy of *fliF*. Electron microscopy showed that LS1218 containing the constructs bearing Δ*2*–Δ*5* did not assemble a flagellum. Together, these results demonstrate

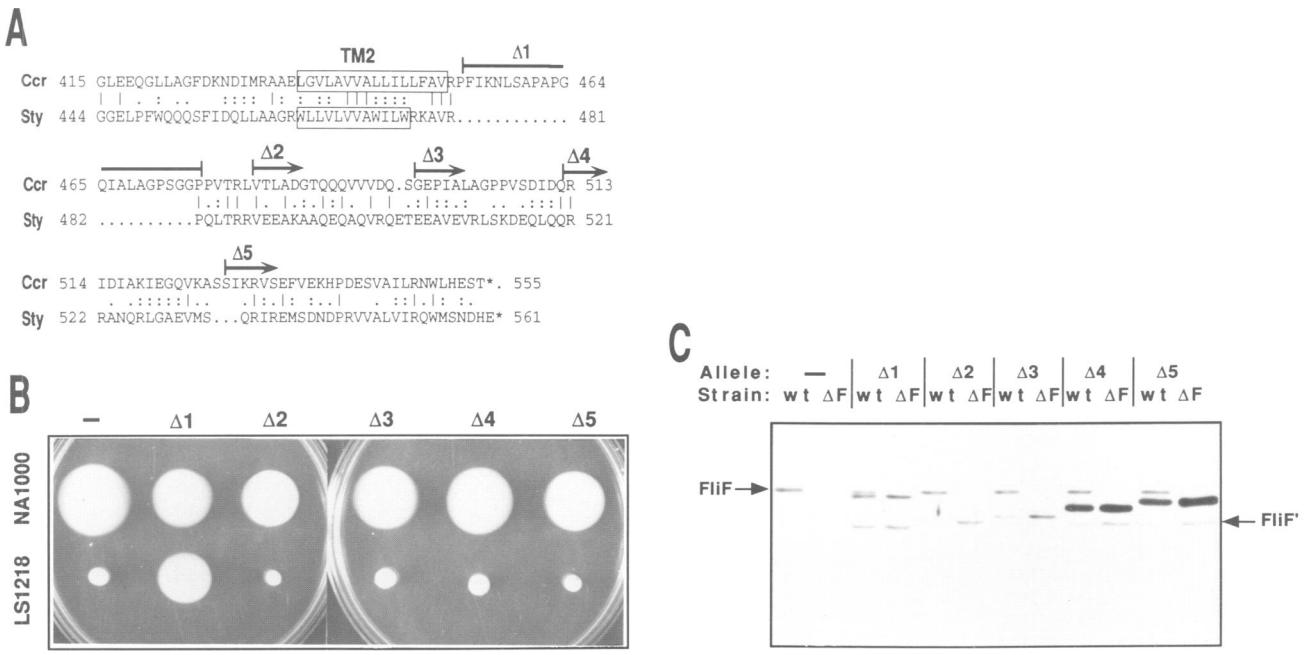

Fig. 5. Genotypes, motility phenotypes and products of *fliF* C-terminal deletions. (**A**) Sequence comparison of the C-termini of FliF from *C.crescentus* (Ccr) and *S.typhimurium* (Sty). The proposed transmembrane-spanning domains (TM2) are boxed, and the in-frame deletions (Δ1–Δ5) are indicated. Δ1 deletes 22 internal amino acids immediately after TM2. Decreasing numbers of amino acids from the C-terminus are deleted in Δ2 (72 amino acids), Δ3 (57 amino acids), Δ4 (41 amino acids) and Δ5 (26 amino acids). (**B**) Swarm agar plate assay used to determine the motility phenotype of *fliF* deletion mutants. Colonies of NA1000 and LS1218 with and without plasmids containing *fliF* deletion alleles Δ1–Δ5 (pUJ99–pUJ103) are shown on semisolid PYE agar (0.3%) plates. Only the plasmid expressing FliF derivative Δ1 (pUJ99) is able to complement the nonmotile phenotype of the *fliF* null mutant LS1218. (C) Immunoblot with the total protein of NA1000 wild type and *fliF* deletion strain (LS1218) carrying plasmids with the *fliF* C-terminal deletion alleles Δ1–Δ5 (pUJ99–pUJ103). The same amounts of protein were separated on a 10% SDS–polyacrylamide gel, transferred to a polyvinylidine difluoride membrane and stained as described in Materials and methods. The FliF wild-type protein, marked by an arrow, is present in *C.crescentus* wild-type strain NA1000 (wt) but absent in the *fliF* null mutant LS1218 (ΔF). The slightly smaller FliF deletion derivatives (51–57 kDa) are expressed from a plasmid (pGL10), and therefore are present in both wild-type and *fliF* null mutant strains. An additional band (FliF′; 51–52 kDa) is observed in extracts of cells carrying the *fliF* alleles on a plasmid corresponding to one of the FliF degradation products resulting from slight overexpression of the FliF deletion derivatives (compare with Figure 2A, lane 3). This band has a constant size when derived from FliF derivatives Δ2–Δ5, corresponding roughly to the size of FliFΔ2. However, the band shifts in size when derived from FliFΔ1, suggesting that it is the result of an endoproteolytic cut at the site coinciding with the C-terminus of FliFΔ2.

that, while the domain immediately following TM2 (Δ*1*) is not required for motility, the C-terminal 20–30 amino acids of FliF are strictly required for motility and flagellar assembly.

Strains carrying the different *fliF* C-terminal deletion alleles were analysed immunologically to detect the FliF deletion derivatives (Figure 5C). One of the two prominent FliF degradation products shown in Figure 2A (lane 3) was also visible in all extracts from strains carrying a plasmid-encoded *fliF* allele (Figure 5C, FliF′). This prominent band is likely to be the product of a nonspecific degradation event caused by slight overexpression of the FliF derivatives. We localized the position of the presumed proteolytic cut leading to this degradation product very close to the Δ*2* deletion site (Figure 5A) in the cytoplasmic C-terminal portion of FliF, based on the facts that (i) all *fliF* alleles (Δ*1*–Δ*5*) produced the FliF′ band, (ii) FliF′ derivatives originating from alleles Δ*2*–Δ*5* had a common size, similar to the molecular weight of the deletion derivative FliFΔ2, and (iii) allele Δ*1* produced a slightly smaller degradation product FliF′ resulting from the internal 22 amino acid deletion (Figure 5C).

The relative levels of the FliF protein lacking either 41 or 26 C-terminal amino acids (Δ*4* and Δ*5*) were significantly higher than that seen with the wild-type protein (Figure 5C). In contrast, deletions of 72 and 57 C-terminal amino acids (Δ2 and Δ3) resulted in relatively lower protein levels, most pronounced when expressed in a wild-type background (Figure 5C). Steady state levels of the FliF derivative lacking 22 internal amino acids (Δ1) were comparable with wild-type levels. The different protein levels suggest different stabilities of the FliF deletion derivatives. To examine the *in vivo* stability of each of these FliF derivatives, pulse–chase experiments were carried out, as described in Materials and methods. The FliF wild-type protein decayed with a half-life of ~60 min and was largely turned over after 3 h (Figure 6). A 3 h period for the complete turnover of FliF was expected because the protein fluctuates during the course of one single cell cycle (Figures 1A and 3) and it takes cells growing on minimal media ~3 h to proceed through one cycle. The FliF derivative with a 72 amino acid C-terminal deletion (Δ2) was too unstable to be detected by immunoprecipitation in this experiment. Similarly, Δ3 (57 amino acid deletion) decayed significantly faster than wild-type FliF, whereas the two deletion derivatives Δ4 and Δ5 showed a substantially increased stability (Figure 6), consistent with the increased steady state protein levels observed in the immunoblots shown in Figure 5C.

Because FliF stability in *C.crescentus* is determined in large part by specific proteolytic turnover during the swarmer-to-stalked cell differentiation (Figure 3), we

Table I. Strains and plasmids

Strain	Genotype	Reference, source
E.coli		
BL21(DE3)	F⁻ *lon ompT* r_B^- m_B^- λDE3	Novagen
DH10B	F⁻ *mcr*A Δ(*mrr hsd*RMS *mcr*BC)Φ80d*lacZ*ΔM15 Δ*lacX*74 *end*A1 *rec*A1 *deo*R Δ(*ara*, *leu*)7697 *ara*D139 *gal*U *gal*K *nup*G *rps*L	Gibco BRL
DH11S	*mcr*A Δ(*mrr hsd*RMS *mcr*BC) Δ(*lac–pro*AB) Δ*rec*A1398 *deo*R *rps*L *srl*⁻*thi*⁻ / F′*pro*AB+ *lac*IqZΔM15	Gibco BRL
S17-1	M294::RP4-2 (Tc::Mu) (Km::Tn7)	Simon *et al.* (1983)
SM10	M294::RP4-2 (Tc::Mu)	Simon *et al.* (1983)
C.crescentus		
NA1000	syn-1000, synchronizable derivative of *C.crescentus* wild-type strain	Evinger and Agabian (1977)
LS107	NA1000*bla6*	Dickon Alley
LS785	NA1000::p1B1	this work
LS786	NA1000::p1P1	this work
LS787	NA1000::p0S5	this work
LS1218	NA1000Δ*fliF*	this work
LS1535	LS107::pUJ49	this work
LS1702	LS107::pUJ73	this work
LS1707	LS1218::pUJ87	this work
LS1534	LS1218/pUJ62	this work
LS1939	NA1000/pUJ99	this work
LS1940	NA1000/pUJ100	this work
LS1941	NA1000/pUJ101	this work
LS1942	NA1000/pUJ102	this work
LS1943	NA1000/pUJ103	this work
LS1944	LS1218/pUJ99	this work
LS1945	LS1218/pUJ100	this work
LS1946	LS1218/pUJ101	this work
LS1947	LS1218/pUJ102	this work
LS1948	LS1218/pUJ103	this work
LS1984	LS1218/pUJ104	this work
LS1987	NA1000::pUJ109	this work
LS1988	NA1000::pUJ110	this work
LS1989	NA1000::pUJ111	this work
LS1992	LS1218::pUJ109	this work
LS1993	LS1218::pUJ110	this work
LS1994	LS1218::pUJ111	this work
LS2252	LS107::pUJ114	this work
LS2356	NA1000Δ*fliG*	this work

Plasmid	Description	Reference, source
p0S5	*fliF/lacZ* translational fusion (at *Sal*I site) in pJBZ280	Kim Quon
p1P1	*fliF/lacZ* translational fusion (at *Pst*I site) in pJBZ281	Kim Quon
p1B1	*fliF/lacZ* translational fusion (at *Bgl*II site) in pJBZ281	Kim Quon
pBluescript SK (+)	Amp^R cloning vector	Stratagen
pDELTA	Kan^R, Amp^R, Tet^R vector containing the *sacB* gene	Gibco BRL
pET-21a	Amp^R vector for protein overexpression	Novagen, Madison, WI
pGL10	Kan^R broad host-range vector	Don Helinski
pJAMY30–32	Kan^R vectors for protein fusions to β-lactamase	Dickon Alley
pJBZ280–282	Kan^R vectors for protein fusions to β-galactosidase	Dickon Alley
pLITMUS28	pUC-based Amp^R cloning vector	New England Biolabs
pMH1701	plasmid containing *nptI–sacB–scaR* cartridge (3.8 kb *Bam*HI)	Hynes *et al.* (1989)
pMR10	Kan^R derivative of pGL10	Chris Mohr and Rick Roberts
pMR20	Tet^R derivative of pGL10	Chris Mohr and Rick Roberts
pNPT228	Kan^R derivative of pLITMUS28 with *oriT*	Dickon Alley
pUJ29	pET21a + 0.9 kb PCR fragment of *fliF*	this work
pUJ49	*fliF–bla* translational fusion (at *Bgl*II site) in pJAMY31	this work
pUJ62	*Bam*HI–*Eco*RI fliF fragment in pGL10	this work
pUJ72	*Bam*HI–*Nco*I *fliF* fragment in pBluescript SK (+)	this work
pUJ73	*fliF–bla* translational fusion (at *Sal*I site) in pJAMY30	this work
pUJ87	*fliF* under the control of the constitutive promoter P*xyl*	this work
pUJ99	*Bam*HI–*Eco*RI fragment of Δ*fliF1* in pMR10	this work
pUJ100	*Bam*HI–*Nco*I fragment of Δ*fliF2* in pMR10	this work
pUJ101	*Bam*HI–*Nco*I fragment of Δ*fliF3* in pMR10	this work
pUJ102	*Bam*HI–*Nco*I fragment of Δ*fliF4* in pMR10	this work
pUJ103	*Bam*HI–*Nco*I fragment of Δ*fliF5* in pMR10	this work
pUJ104	*Bam*HI–*Nco*I fragment of *fliF* in pMR20	this work
pUJ105	*Nco*I–*Eco*RV fragment containing part of *fliG* in pLITMUS28	this work
pUJ106	*Spe*I–*Afl*II fragment containing part of *fliG* from pUJ105 in pNPT228	this work
pUJ109	*fliF–fliG* translational fusion in pNPT228	this work
pUJ110	Δ*fliF4–fliG* translational fusion in pNPT228	this work
pUJ111	Δ*fliF5–fliG* translational fusion in pNPT228	this work
pUJ114	*fliF–bla* translational fusion (at *Pst*I site) in pJAMY31	this work

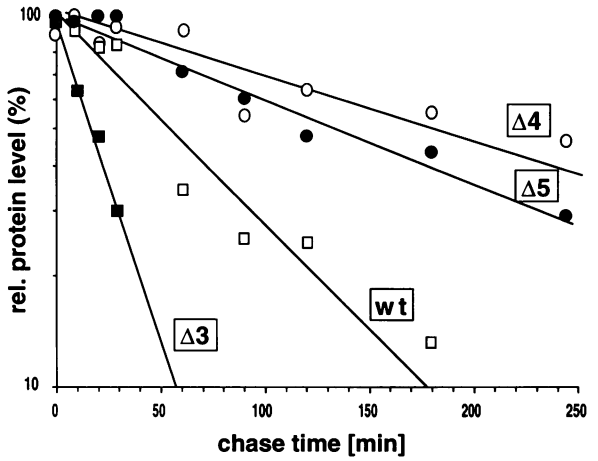

Fig. 6. Stability of FliF wild-type and C-terminal deletion derivatives. The stability of FliF wild-type protein (wt) and FliF deletion derivatives (Δ3–Δ5) was determined in pulse–chase experiments (see Materials and methods). Mixed cell populations of LS1946 (LS1218/pUJ101; FliFΔ3), LS1947 (LS1218/pUJ102; FliFΔ4), LS1948 (LS1218/pUJ103; FliFΔ5) and LS1984 (LS1218/pUJ104; wild-type FliF) were labelled and chased for increasing amounts of time. The FliF protein was immunoprecipitated from lysed cell extracts. Protein levels were determined quantitatively from autoradiographs with a PhosphorImager, and numbers were plotted as a percentage of the highest value.

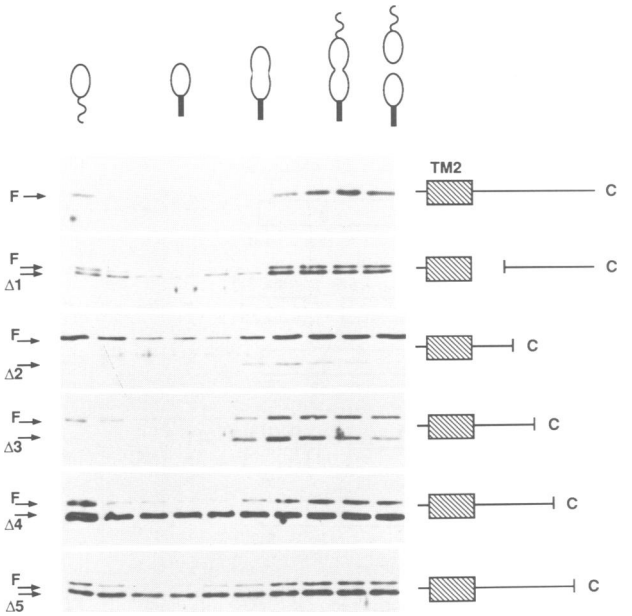

Fig. 7. Cell cycle-dependent proteolysis of FliF and its C-terminal deletion derivatives. Steady state levels of the FliF wild-type protein and C-terminal deletion derivatives were determined in synchronized *C.crescentus* populations throughout the cell cycle. Immunoblots of cell extracts of (from top) NA1000, LS1939 (NA1000/pUJ99; Δ1), LS1940 (NA1000/pUJ100; Δ2), LS1941 (NA1000/pUJ101; Δ3), LS1942 (NA1000/pUJ102; Δ4) and LS1943 (NA1000/pUJ103; Δ5) were stained with the FliF-specific antibody. The chromosomally encoded FliF wild-type protein (upper band in each panel) is used as an internal turnover control in strains expressing FliF deletion derivatives Δ1–Δ5 (lower band) from a plasmid. The corresponding bands are marked by an arrow on the left, the identity of the C-terminus of each FliF derivative is indicated schematically on the right, and progression through the cell cycle is shown above the panels.

determined if the increased overall stability of Δ4 and Δ5 was the result of a loss of cell cycle-specific proteolysis. Steady state levels of the different FliF derivatives were followed throughout the cell cycle by an immunoblot analysis (Figure 7). The FliF deletion derivatives Δ1–Δ5 were expressed from plasmids in a *C.crescentus* wild-type strain, allowing us to monitor the chromosomally encoded FliF wild-type protein as an internal control. The turnover of Δ1 was similar to the FliF wild-type protein (Figure 7, Δ1). The derivatives Δ2 and Δ3 were only detectable in the predivisional cell (when FliF was actively synthesized) but were not observed in swarmer cells (Figure 7, Δ2 and Δ3). This reflects the overall instability of these FliF mutant proteins that lack most of their cytoplasmic C-terminus. However, the levels of the two deletion derivatives Δ4 and Δ5 remained constant during the swarmer-to-stalked cell transition, while the wild-type protein was degraded normally in the same cells (Figure 7, Δ4 and Δ5). We conclude that the C-terminus of FliF is required for cell cycle-dependent proteolytic turnover.

Interaction between the FliF membrane MS-ring protein and the cytoplasmic FliG switch protein

In *S.typhimurium*, the FliG switch protein is localized to the cytoplasmic face of the transmembrane MS-ring (Figure 1B) because of a direct interaction of the FliF C-terminus with the N-terminus of the FliG switch protein (Francis *et al.*, 1992). Deletion of the C-terminus of the *C.crescentus* FliF protein could, therefore, lead to a disruption of its interaction with FliG, and consequently to a failure in flagellar assembly. To test this hypothesis, and to investigate whether such a morphogenetic defect is responsible for the lack of cell cycle turnover of the FliF protein, we asked if fusion proteins between the stable FliF mutant derivatives and the FliG switch protein could restore these functions. The FliF wild-type protein and the FliF deletion derivatives Δ4 and Δ5 were fused to the FliG protein at position Met49, resulting in the deletion of 48 N-terminal amino acids of FliG. A linker of 13 amino acids was introduced between the FliF and FliG parts of the fusion (Figure 8A). The genes encoding these fusion proteins were crossed into the chromosome of the *fliF* null mutant strain LS1218 by homologous recombination, and the resulting strains were tested for the presence of the fusion proteins as well as for motility, cell division and the cell cycle-regulated proteolysis of FliF.

An immunoblot analysis confirmed the presence of the three fusions between FliF, Δ4, Δ5 and the truncated FliG (Figure 8B; FG′, FΔ4G′ and FΔ5G′) in their respective strains. Fusions of the FliF derivatives Δ4 and Δ5 to FliG restored swimming to the *fliF* null strain. However, fewer cells were swimming, and those that were, were unable to reverse the direction of their movement (Figure 8A). This suggests that a FliF–FliG fusion protein assembled into a basal body structure permits motor function but is unable to switch the direction of its rotation. More importantly, these results strongly suggest that FliF and FliG interact via their respective C- and N-termini, and that this interaction is essential for flagellar assembly. In support of this, we found that the nonmotile C-terminal deletion mutants *Δ4* and *Δ5* caused a strong filamentous phenotype similar to that reported for the *fliF* null mutant

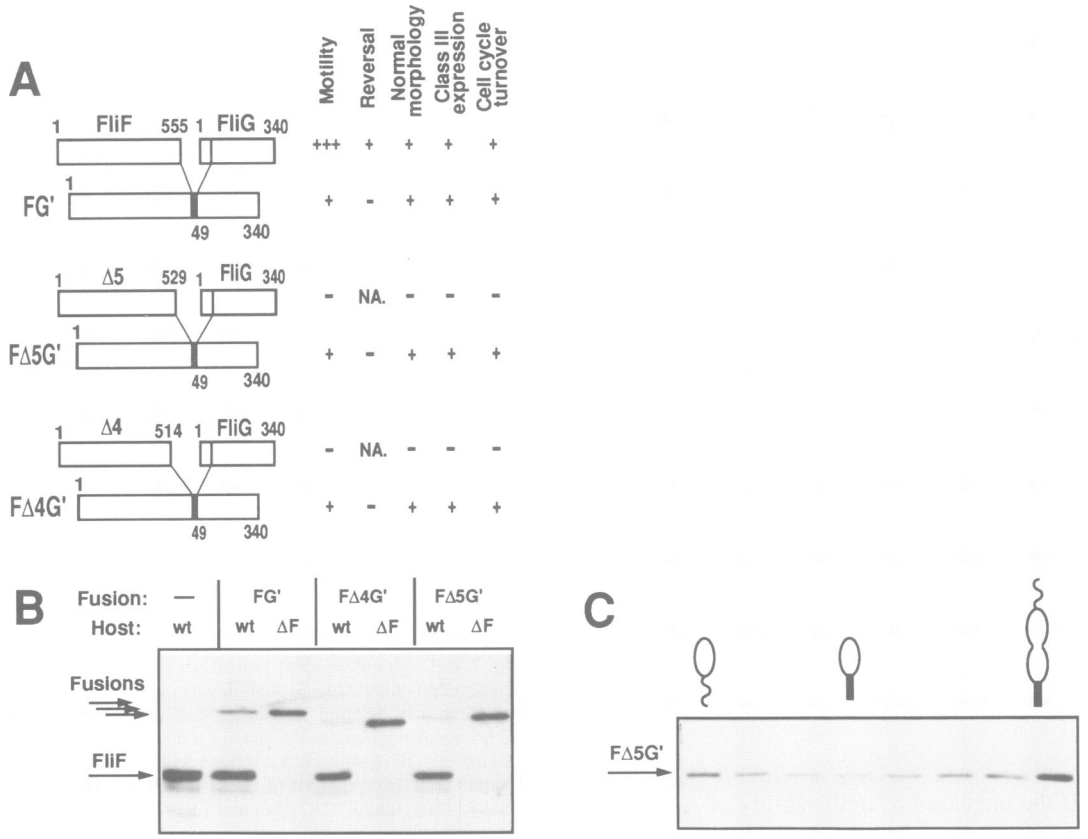

Fig. 8. Fusion of FliG to FliF C-terminal deletion derivatives restores motility, proper cell division and cell cycle proteolysis. (**A**) FliF wild-type protein and deletion derivatives Δ4 and Δ5 were fused in-frame to the switch protein FliG. The C-terminus of FliF (position 555 for wild type, position 529 for Δ5 and position 514 for Δ4) was fused to amino acid 49 of FliG, resulting in a truncated FliG protein (G′). A 13 amino acid linker (black bar) was introduced between the FliF and FliG portions of the fusions. The genes coding for the three fusion proteins FG′ (FliF–FliG), FΔ4G′ (Δ4–FliG) and FΔ5G′ (Δ5–FliG) were introduced into the chromosome of the *fliF* null mutant strain LS1218. The resulting strains (LS1992–1994) were analysed for their phenotype: the motility and morphology (cell division) were analysed microscopically; the expression of Class III flagellar genes was examined by immunoblots using a FlgH-specific antibody; and cell cycle turnover of the fusion proteins was tested immunologically in synchronized cultures using an antibody specifically recognizing FliF (see Figure 8C). The motility of the strains containing the fusion proteins was reduced (+) compared with wild type (+++) in that fewer cells were swimming. The phenotypes of strains carrying the fusion proteins (rows 2, 4 and 6) are compared with a wild-type strain (row 1) and strains containing the FliF deletion derivatives Δ5 (LS1948; row 3) and Δ4 (LS1947; row 5). (**B**) Immunoblot analysis of *C.crescentus* wild-type strain NA1000 (wt) and of *fliF* null mutant strain LS1218 (ΔF) expressing the FliF–FliG fusions. Plasmids pUJ109 (FG′), pUJ110 (FΔ4G′) and pUJ111 (FΔ5G′) were introduced into the chromosome of NA1000 (strains LS1987–1989) and LS1218 (strains LS1992–1994). Equal amounts of total protein of each of these strains were separated in each lane and stained with the FliF-specific antibody. The host strain and the fusion expressed by each strain are indicated. The bands corresponding to the FliF wild-type protein and to the three fusion proteins are marked by arrows. (**C**) Cell cycle-dependent proteolysis of the FΔ5G′ fusion protein. Strain LS1994 (LS1218::pUJ111) was analysed immunologically for steady state levels of the FΔ5G′ fusion protein throughout the cell cycle using the FliF-specific antibody. The stages of the cell cycle are indicated schematically.

(see Materials and methods) and did not express Class III flagellar genes. Both phenotypes were completely reversed upon fusion of these FliF derivatives to FliG (Figure 8A). This confirms that the FΔ4G′ and FΔ5G′ fusion proteins are able to assemble the first flagellar checkpoint structure (Ramakrishnan *et al.*, 1994).

Both fusion proteins FΔ4G′ and FΔ5G′, although lacking the FliF turnover determinant, were degraded during the swarmer-to-stalked cell transition (shown for FΔ5G′, Figure 8C). This suggests that there is either an independent turnover determinant in FliG or a requirement for a FliF–FliG complex for degradation. To distinguish between these two possibilities, we generated an in-frame deletion of the chromosomal copy of *fliG*. If FliF–FliG interaction is indeed required for the cell cycle degradation of FliF, a disruption of *fliG* should cause a stable FliF protein. In fact, FliF degradation during the swarmer-to-stalked cell transition in the *fliG* null strain was indistinguishable from turnover in the wild-type strain (Figure 9). Therefore, these experiments suggest that FliG might have a turnover determinant that allows the FliF–FliG fusion to be degraded during the swarmer-to-stalked cell transition.

FliF is segregated to the swarmer pole independent of FliF proteolysis

The earliest assembled structural components of the flagellum (encoded by Class II flagellar genes) are expressed early in the predivisional cell when the swarmer and stalked cell compartments have not yet been established. The products of Class II flagellar genes are thought to be targeted to the site of their assembly at the swarmer pole of the predivisional cell, and upon division to appear only in the progeny swarmer cell. We analysed FliF distribution in the newly formed daughter cells (Figure 10A). As described in Materials and methods, a synchronized

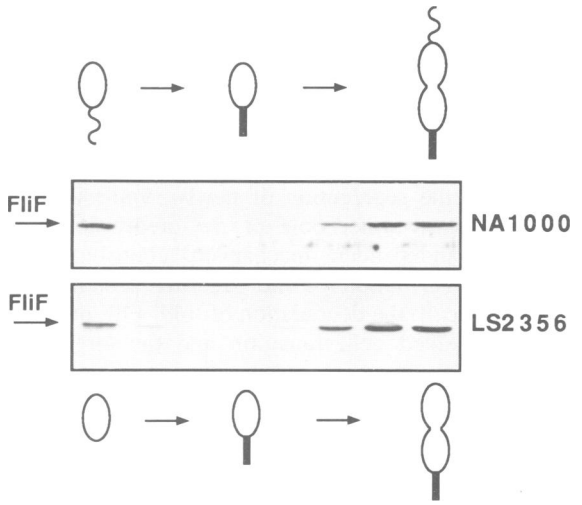

Fig. 9. Cell cycle-dependent proteolysis of FliF in a *fliG* deletion mutant. Steady state levels of the FliF protein were determined in synchronized *C.crescentus* wild-type (NA1000) and Δ*fliG* (LS2356) populations throughout the cell cycle. Immunoblots of cell extracts from NA1000 and LS2356 were stained with the FliF-specific antibody. Cells containing the *fliG* deletion were slightly filamentous when grown on M2G minimal medium and did not assemble a flagellum (data not shown). The stages of the cell cycle are indicated schematically.

population of cells was allowed to proceed through the cell cycle, and progeny swarmer and stalked cells were separated after cell division. An immunoblot analysis of swarmer and stalked cell fractions revealed that FliF was present predominantly in swarmer cells (Figure 10A). We also assayed the presence of one of the switch proteins, FliM (Figure 1B), following cell division. Like FliF, FliM was found mainly in swarmer cells following cell division (Figure 10A), supporting the contention that Class II flagellar components are targeted to the swarmer pole.

How do these proteins choose the swarmer pole of the predivisional cell? One possibility is that they can distinguish between the identity of the stalked pole and its antipode, where the flagellar structure is going to be assembled. Alternatively, early flagellar proteins could be equally distributed to both poles of the predivisional cell but then be selectively degraded at the stalked pole. Stable FliF derivatives (Δ4 and Δ5) lost their bias to the swarmer cell (Figure 10A). However, this apparent loss of asymmetry could be a consequence of incomplete FliF proteolysis during the swarmer-to-stalked cell transition and not due to the initial targeting event. Persistent FliF protein at the new stalked pole would end up in the newborn stalked cell. To test this, newly synthesized FliF protein was pulse labelled in predivisional cells and chased until the daughter cells were completely separated (Figure 10B). The distribution of the labelled FliF protein in the two daughter cell types was then determined by immunoprecipitation. As expected, the labelled FliF wild-type protein segregated to the swarmer cell (Figure 10B). However, we found that the stable 26 amino acid C-terminal deletion derivative of FliF (Δ5) also exhibited a strong bias towards the swarmer progeny (Figure 10B). Thus, localization of the newly synthesized FliF protein to the swarmer pole was not dependent on its proteolytic removal at other sites, but the maintenance of asymmetry was dependent

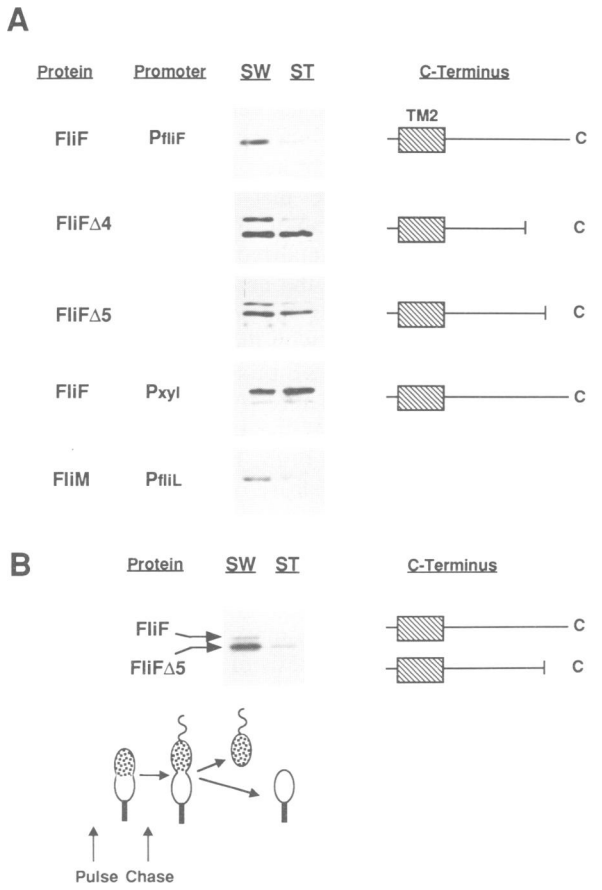

Fig. 10. Segregation of the MS-ring protein to the swarmer pole of the predivisional cell. The distribution of FliF in the progeny swarmer and stalked cells was analysed by immunoblots (A) and immunoprecipitation (B). (**A**) Newly divided swarmer (SW) and stalked cells (ST) were separated as described in Materials and methods. Equal amounts of total protein were analysed in an immunoblot with FliF- or FliM-specific antibodies. The detected protein and the promoter that drives the gene coding for the corresponding protein are indicated to the left. P*xyl* is a constitutive promoter induced by xylose (A.Meisenzahl, L.Shapiro and U.Jenal, unpublished data). The following strains were used to express these proteins: NA1000 (FliF, FliM), LS1942 (NA1000/pUJ102; Δ4), LS1943 (NA1000/pUJ103; Δ5) and LS1707 (LS1218::pUJ87). The C-terminus of the analysed FliF derivatives is shown schematically on the right. (**B**) Predivisional cells of strain LS1943 (NA1000/pUJ103) were pulse labelled and chased until cell division was completed (shown diagrammatically). The two cell types were separated as described, and equal amounts of labelled protein from the swarmer and stalked fractions were then used for immunoprecipitation with the FliF-specific antibody. Strain LS1943 expresses the FliF wild-type protein from the chromosome and the FliFΔ5 derivative from plasmid pUJ103. The precipitated proteins are marked to the left, and their C-termini are indicated to the right. Segregation of the FliF protein to the swarmer pole of the predivisional cell is indicated in the schematic representation of the different cell types.

on FliF proteolysis during the swarmer-to-stalked cell transition.

Discussion

The *C.crescentus* polar flagellum is a complex macromolecular structure that is assembled at one cell pole and later released during each cell cycle. The cell cycle control of flagellar biogenesis requires the timed expression of flagellar components, while the positioning of the flagellum

to the swarmer pole of the predivisional cell demands a specific targeting mechanism for the flagellar proteins. An understanding of how the FliF protein is targeted to the cell pole of the predivisional cell is important for a definition of the specific mechanisms used to initiate flagellar biogenesis, and for protein localization in bacteria in general. We show here that a key component of the *C.crescentus* flagellar motor, the MS-ring protein, is synthesized and compartmentalized during the S phase of the cell cycle, and later, in the next G_1 phase, is proteolytically removed. Synthesis and segregation of the MS-ring protein, FliF, coincide with the initiation of flagellar assembly at the cell pole; FliF proteolysis coincides with release of the flagellar structure. A flagellum fails to be assembled in the absence of the FliF protein. Thus, the temporal and spatial control of the FliF protein are critical steps in the assembly and release of the flagellum.

Newly synthesized FliF segregates to the swarmer pole of the predivisional cell

We have shown here that newly synthesized FliF protein segregates to the swarmer compartment of the predivisional cell. Because the synthesis of FliF takes place long before two compartments have formed in the predivisional cell, localized transcription, as shown for some of the Class III and IV flagellar genes (Gober *et al.*, 1991; Wingrove *et al.*, 1993), can be excluded as a targeting mechanism. Rather, the FliF protein itself must be sequestered to the swarmer pole of the predivisional cell, where it is assembled into the first ring structure of the flagellar motor.

Studies in the multiflagellated bacterium *S.typhimurium* have shown that the MS-ring structure is formed in the cytoplasmic membrane independent of any other known flagellar genes, with the exception of the regulatory master operon (Kubori *et al.*, 1992), strongly suggesting that FliF polymerization occurs at the beginning of the assembly process. Labelling studies with ts flagellar mutants support this finding, and further suggest that FliF and the FliG switch protein at the cytoplasmic face of the membrane might be coassembled (Jones and Macnab, 1990). Therefore it is likely that FliF alone, or in a complex with one or more early flagellar proteins, is targeted to the swarmer pole of the *C.crescentus* predivisional cell, thereby initiating the localized assembly process.

The chemoreceptor McpA is targeted to the swarmer pole of the *C.crescentus* predivisional cell and is proteolytically turned over during differentiation of the swarmer pole into a stalked pole (Alley *et al.*, 1992, 1993). A McpA chemoreceptor lacking 30 amino acids at its C-terminus was not turned over during the swarmer-to-stalked cell transition, and was then found at both the swarmer and stalked poles of the predivisional cell. Thus, proteolysis during the swarmer-to-stalked cell transition contributes to the maintenance of the asymmetric distribution of McpA (Alley *et al.*, 1993). Similarly, stable FliF derivatives lacking portions of their C-terminus lose the apparent asymmetric distribution to the swarmer compartment. However, the immunoblots used in our study, or immunoelectron microscopy used by Alley *et al.* (1993), do not distinguish between protein synthesized *de novo* in the predivisional cell and protein left over from the last cell cycle because of lack of turnover. This was resolved by analysing the distribution of newly synthesized FliF protein in the predivisional cell. It was found that both FliF wild-type protein and a stable FliF C-terminal deletion derivative synthesized in the predivisional cell segregated preferentially to the swarmer compartment. Therefore we conclude that stalked pole-specific proteolysis does not contribute to the segregation of newly synthesized FliF protein to the swarmer pole of the predivisional cell, but that two independent mechanisms contribute to the asymmetric distribution of the MS-ring protein in the predivisional cell: the degradation of 'old' FliF during the swarmer-to-stalked cell transition and the targeting of 'new' FliF to the swarmer pole of the predivisional cell.

Cell cycle-dependent degradation of the MS-ring protein

It is becoming increasingly apparent, in all biological systems, that temporally controlled proteolysis plays a key role in cell cycle control and in differentiation and development. For example, cyclins are short-lived eukaryotic proteins whose programmed degradation at specific stages of the cell cycle is essential for normal progression of the cell cycle (Glotzer *et al.*, 1991; King *et al.*, 1994). Little information is available in prokaryotes about regulated proteolysis in general, and about cell cycle-regulated proteolysis in particular. The *Escherichia coli* regulatory protein LexA is inactivated by cleavage in response to DNA damage. LexA cleavage is catalysed by a cryptic protease activity and is dependent on the RecA protein that has to be activated by a DNA damage-induced signal (Little *et al.*, 1980; Horii *et al.*, 1981). Another example is the heat-shock sigma factor of *E.coli*, sigma 32, that accumulates after temperature upshift, partly through a transient protein stabilization. The cooperative interaction of molecular chaperones DnaK, DnaJ and GrpE with the heat-shock sigma factor is involved in its regulated proteolysis (Tilly *et al.*, 1989; Straus *et al.*, 1990; Gamer *et al.*, 1992; Liberek *et al.*, 1992, 1995; Liberek and Georgopoulos, 1993; Nagai *et al.*, 1994), and a membrane-bound protease, FtsH, has recently been shown to degrade sigma 32 in an ATP-dependent manner (Herman *et al.*, 1995; Tomoyasu *et al.*, 1995).

We have presented evidence that the flagellar MS-ring protein is specifically degraded during the swarmer-to-stalked cell transition and have shown that FliF levels rise later in the cell cycle when FliF synthesis is resumed. The degradation of FliF coincides with release of the flagellum, perhaps providing a clue to the physiological relevance of FliF proteolysis. Flagellar release is an integral part of the developmental program that controls the differentiation of a swarmer cell into a stalked cell. There are several observations that support the contention that cell cycle proteolysis controls flagellar release and that the MS-ring is a likely substrate of this developmental event. During the normal cell cycle, a complex composed of filament, hook and rod is released into the culture fluid (Shapiro and Maizel, 1973; Stallmeyer *et al.*, 1989a), and the break in the structure occurs at the junction between a proximal and a distal portion of the rod (Stallmeyer *et al.*, 1989a). Recent studies on the domain structure of the *S.typhimurium* MS-ring protein have shown that the FliF protein assembles into a structure consisting of the M-ring, the S-ring and a short rod-like extension (Ueno *et al.*, 1992,

1994), the latter most likely corresponding to the proximal rod portion observed in *C.crescentus*. The observed break resulting in the release of the flagellum is therefore in very close proximity to the structure formed by the FliF protein. Furthermore, because the MS-ring anchors the flagellar structure in the cytoplasmic membrane, proteolysis of FliF would automatically result in release of the attached distal components of the flagellum. Additional information about flagellar anchoring and release comes from studies of a *S.typhimurium fliF* mutant that exhibits an increase in detached filaments when grown in viscous media. It is relevant that the filaments released from this mutant had the hook and part of the rod still attached, suggesting that the mutant FliF protein causes a fragile MS-ring–rod connection leading to the observed release of the rod–hook–filament complexes (Okino *et al.*, 1989).

The FliF C-terminus is required for flagellar assembly and contains a determinant for cell cycle turnover of the MS-ring protein

Short C-terminal deletions disrupt the cell cycle-specific degradation pattern of FliF. These deletion derivatives also fail to assemble a flagellum. Thus, the C-terminus of FliF contains determinants for both flagellar assembly and FliF turnover. The requirement of the FliF C-terminus for flagellar assembly appears to be because of its interaction with the FliG switch protein located at the cytoplasmic face of the cell membrane. A fusion between the truncated FliF derivatives and FliG partially restored the motility phenotype of the *fliF* deletion mutants. In addition, protein fusion fully restored the regulatory features of the first flagellar checkpoint. A structural intermediate composed of proteins encoded by Class II flagellar genes is thought to regulate both the expression of late flagellar genes and progression through the cell cycle (Jenal *et al.*, 1994; Ramakrishnan *et al.*, 1994). The MS-ring is a central component of this first checkpoint structure; a *fliF* null mutant is defective in late flagellar gene expression and has a strong cell division phenotype. Both cell division and the expression of FlgH, an outer ring protein encoded by a Class III flagellar gene, were found to be complemented by fusing nonfunctional FliF deletion mutants to FliG. Together, these results strongly suggest that the FliF–FliG fusions, lacking 26 or 41 amino acids of the FliF C-terminus, are assembled into a partially functional motor structure that has all the regulatory properties of the first checkpoint structure. FliF–FliG fusions generated in *S.typhimurium* behave similarly: strains containing either a full-length fusion between FliF and FliG, or a fusion which deleted 56 amino acids from the FliF C-terminus and 94 amino acids from the FliG N-terminus, were partially motile and the fusion proteins were detected in biochemically isolated basal body–hook complexes (Francis *et al.*, 1992). In addition, *in vitro* binding studies with purified proteins have shown that FliF interacts with both the FliG and FliM switch proteins (Oosawa *et al.*, 1994).

Although C-terminal deletions of FliF result in the loss of FliF proteolysis during the swarmer-to-stalked cell transition, cell type-specific proteolysis is restored if these deletion derivatives are fused to FliG. Wild-type FliF is degraded normally in the absence of FliG, ruling out the possibility that FliF is turned over only when it is in complex with FliG. This suggests that FliG is also subject to cell cycle-controlled proteolysis, as has been shown for another switch protein, FliM (Jenal *et al.*, 1994). Although we cannot rule out the possibility that the interaction of the FliF C-terminus with an unknown protein is the signal for cell cycle turnover of the MS-ring, it is more likely that the C-terminus of FliF contains a turnover determinant that tags the protein for degradation at a specific stage of the cell cycle. This can occur through direct recognition of this part of the protein by a specific protease or through a modification of this domain that converts the protein into a proteolytic substrate. A comparison of the amino acid sequences of the FliF C-terminus and the switch proteins FliG and FliM did not reveal any common primary sequence domains, although a conserved secondary structure remains a possible common determinant.

The flagellar MS-ring protein and the McpA chemoreceptor protein are degraded concomitantly during the *C.crescentus* cell cycle (Alley *et al.*, 1993; this study). Both proteins are specifically localized to the swarmer pole of the predivisional cell and are thereby confined to the newborn swarmer cell (Alley *et al.*, 1992; this study). FliF and McpA have similar membrane topologies with two membrane-spanning domains and both the N- and the C-termini localized in the cytoplasm. Cell cycle degradation of both proteins requires a domain at the C-terminus (Alley *et al.*, 1993; this study). Therefore it is possible that the cell cycle-dependent degradation of FliF and McpA is the result of similar or identical molecular mechanisms. However, no common sequence motifs could be identified in the C-termini of the FliF and McpA proteins, leaving the possibility that structural similarities of the C-termini could contribute to recognition by the same proteolytic machinery. Some examples exist for C-terminal stability determinants: a tail-specific ATP-independent protease (Tsp) was identified in *E.coli* that preferentially degrades proteins with a hydrophobic tail (Parsell *et al.*, 1990; Silber *et al.*, 1992). Tsp is identical to Prc, a protein that is involved in the C-terminal processing of penicillin-binding protein 3 (Hara *et al.*, 1991). The constitutive degradation of mouse ornithine decarboxylase, a highly unstable metabolic enzyme, depends on a PEST sequence at its C-terminus (Ghoda *et al.*, 1989, 1990, 1992; Loetscher *et al.*, 1991). However, no PEST sequences have been found in unstable proteins of bacterial cells.

The protease(s) responsible for the degradation of FliF or McpA has yet to be identified. Given the fact that the degradation of both FliF and McpA requires a cytoplasmic domain, it seems appropriate to expect such a protease to be localized in either the cytoplasm or the inner membrane. We expect that the activity of this protease is restricted to the G_1 phase of the *C.crescentus* cell cycle. Recently, the gene coding for a homologue of the *E.coli* ATP-dependent Lon protease has been isolated in *C.crescentus* (R.Wright, C.Stephens, G.Zweiger, L.Shapiro and M.R.K.Alley, manuscript in preparation). A strain containing an inactivated chromosomal copy of *lon* showed that Lon is not involved in the cell cycle-dependent degradation of FliF and McpA (M.R.K.Alley, U.Jenal and L.Shapiro, unpublished results).

Materials and methods

Strains, plasmids, media, enzymes and chemicals

The strains and plasmids used in this study are listed in Table I. *E.coli* strains were grown at 37°C in LB or superbroth (Sambrook *et al.*, 1989), supplemented with ampicillin (100 μg/ml), carbenicillin (100 μg/ml), kanamycin (30 μg/ml) or tetracycline (10 μg/ml), as necessary. *Caulobacter crescentus* strains were grown at 30°C in either PYE complex medium or M2 minimal glucose medium (M2G; Ely, 1991), supplemented with nalidixic acid (20 μg/ml), tetracycline (1 μg/ml) or kanamycin (20 μg/ml), where indicated.

A horseradish peroxidase (HRP) conjugate of goat anti-rabbit IgG was purchased from Boehringer Mannheim (Indianapolis, IN), formalin-fixed Staph A cells from Gibco BRL (Gaithersburg, MD), uranyl acetate from Ted Pella, Inc. (Redding, CA), Immobilon P membrane from Millipore (Bedford, MA), Renaissance Western Blot chemiluminescence reagent from DuPont NEN (Boston, MA), restriction enzymes from Boehringer Mannheim or New England Biolabs (Beverly, MA) and the resin for the purification of His-tagged proteins from Novagen (Madison, WI). Kits for the isolation and purification of plasmid DNA were obtained from Promega (Madison, WI), Qiagen (Chatsworth, CA) or Schleicher and Schuell (Keene, NH).

Overexpression and purification of FliF–His fusion protein and generation of antibodies

A fragment of the *fliF* gene encoding amino acids 55–349 was generated by PCR and cloned into pET-21a, resulting in the plasmid pUJ29. This vector creates an in-frame fusion between the cloned *fliF* fragment and both an N-terminal T7 epitope tag and a C-terminal His tag. A DNA sequence analysis verified that the fusions between *fliF* and the tags were in-frame.

To induce expression of the *fliF* fusion gene in *E.coli*, the plasmid pUJ29 was transformed into *E.coli* strain BL21(DE3) (Novagen). A culture of strain BL21/pUJ29 was grown to an OD_{600} of 1.0 and then IPTG was added to a final concentration of 1 mM. The fusion on pUJ29 is under the transcriptional control of the T7 promoter. T7 RNA polymerase, encoded on the chromosome of BL21(DE3), is under the transcriptional control of the *lac* promoter. Induction of this promoter with IPTG leads to activation of the T7 promoter by the newly synthesized T7 RNA polymerase, and thereby to expression of the fusion protein. Some 3 h after induction, the fusion protein reached its maximal level of expression and the cells were harvested by centrifugation. The His tag allowed the fusion protein to be affinity purified using a Sephadex nickel column (Jenal *et al.*, 1994). The purified fractions were then separated on a preparative SDS–polyacrylamide gel and the band corresponding to the FliF–His fusion protein was cut out. The polyacrylamide matrix was crushed with a piston, mixed with Freund's adjuvant and used directly to immunize rabbits. Immunization and sampling of the serum were performed by Josman Laboratories (Napa, CA).

Construction of in-frame deletions in the chromosomal copies of fliF and fliG

An in-frame deletion in *fliF* was generated by digesting plasmid pUJ41 with *Bst*BI and *Acc*I and religating the two created overhanging ends. pUJ41 carries a *Bam*HI–*Nco*I insert containing the entire *fliF* and part of the *fliG* gene. Deletion of the *Bst*BI–*Acc*I fragment resulted in an in-frame deletion of 507 internal amino acids of FliF in plasmid pUJ42 (Figure 5). The *Bam*HI–*Nco*I fragment containing the *fliF* deletion was then cloned from pUJ42 into plasmid pUJ1, where it substitutes the *fliF* wild-type copy. The resultant construct pUJ43 contained additional flanking DNA around the *fliF* deletion. Finally, an *Eco*RI–*Pst*I fragment containing the *fliF* deletion and flanking DNA was cloned from pUJ43 into plasmid pDELTA (Gibco BRL), resulting in construct pUJ44. pDELTA derivatives are unable to replicate in *C.crescentus* and contain genes for positive (kanamycin and tetracycline resistance) and negative selection (sucrose sensitivity). pUJ44 plasmid DNA was electroporated into *C.crescentus* wild-type strain NA1000; plasmid integrants into the chromosome were identified by selection for kanamycin-resistant colonies. Second recombination events (loss of the plasmid) were selected by plating colonies on PYE plates containing 3% sucrose. Sucrose-resistant colonies were tested for loss of the antibiotic markers and for loss of motility on semisolid PYE agar (3%) plates. Nonmotile colonies were then tested for chromosomal deletions by a Southern blot analysis. A strain containing a positive clone was selected and named LS1218.

Strain LS1218 did not express the FliF protein (Figure 2A, lane 2), was completely nonmotile, as demonstrated by its inability to spread on semisolid agar plates, and did not assemble a flagellum. The addition of an extrachromosomal copy of the *fliF* gene resulted in synthesis of the FliF protein (Figure 2A, lane 3) and complementation of the motility defect. When grown on complex medium, the mutant forms long filamentous cells reaching up to 20 times the normal cell length. These filamentous cells often had terminally differentiated stalked poles at both ends, suggesting that the Δ*fliF* mutation did not hinder pole development. In addition, positional defects occurred at an increased frequency, in that stalks were grown at lateral positions as well as at the normal polar sites. However, the mutant strain showed no growth disadvantage when the increase of cell mass over time was compared with wild type. An extrachromosomal copy of *fliF* was able to complement the cell division phenotype. We conclude that the Δ*fliF* mutation affects one or several steps of cell division, similar to that observed in strains carrying mutations in other Class II flagellar genes (Yu and Shapiro, 1992; Zhuang and Shapiro, 1995).

A *fliG* deletion was generated by subcloning a *Bgl*II–*Eco*RI fragment from pGIR230 (Ramakrishnan *et al.*, 1994), containing a *fliG* in-frame deletion and flanking regions, into plasmid pNPTS138. The resulting construct pUJ151 was then introduced into *C.crescentus* by conjugation, forcing the plasmid to integrate into the chromosome at the *fliG* locus. Screening for second recombinations resulting in exchange of the chromosomal *fliG* wild-type copy with the *fliG* in-frame deletion was performed as outlined above for the *fliF* deletion and resulted in the generation of strain LS2356.

Construction of FliF C-terminal deletion derivatives and FliF–FliG fusions

The C-terminal deletions in *fliF* were generated by site-directed mutagenesis. For Δ*fliF*1, the primer FliFΔP22G (5′-CCGCGTGACGGGCGGACGGACCGCGAACAA) was used to generate a deletion of 66 bp in the region coding for the FliF C-terminus (pUJ69). The deletion alleles Δ*fliF*2–5 were generated by introducing *Sal*I or *Xho*I sites in the *fliF* 3′ end region (pUJ90–93), and subsequently deleting the DNA fragments between the new sites and the *Sal*I site situated at the 3′ end of *fliF* by restriction digest and religation (pUJ94–97). The primers used were FliF–Sal1 (5′-TCCGCCAGCGTCGACAGCCGCGTGACG) for Δ*fliF*2, FliF–Sal2 (5′-AGCGCGATCGGTTCAGTCGACTGATCGACCACC) for Δ*fliF*3, FliF–Sal3 (5′-TGGCGATGTCGATACTCGAGTCGATGTCGCTGAC) for Δ*fliF*4 and FliF–Sal4 (5′-CACGCGCTTGGTCGACGAGGC) for Δ*fliF*5. The five deletion alleles were then cloned from pUJ69 and pUJ94–97 into the broad host-range vector pMR10, resulting in the new constructs pUJ99 (Δ*fliF*1), pUJ100 (Δ*fliF*2), pUJ101 (Δ*fliF*3), pUJ102 (Δ*fliF*4) and pUJ103 (Δ*fliF*5). These plasmids were introduced by conjugation into NA1000 wild-type strain (LS1939–LS1943) and LS1218, the *fliF* null mutant (LS1944–LS1948).

For the construction of FliF–FliG fusion proteins, a *Nco*I–*Eco*RV fragment containing a large part of *fliG*, including its 3′ end, was cloned into the *Nco*I–*Stu*I sites of pLITMUS28, resulting in construct pUJ105. *fliG* was then subcloned as a *Spe*I–*Afl*II fragment containing the polylinker of pLITMUS from pUJ105 into vector pNPT228, resulting in construct pUJ106. pUJ106 contains transfer functions from pNPT228 and a truncated *fliG* gene that codes for the entire FliG protein, except for its 48 N-terminal amino acids. *Spe*I–*Sal*I fragments were then cloned from pUJ72 (*fliF*), pUJ92 (Δ*fliF*4) and pUJ93 (Δ*fliF*5) into the *Spe*I–*Sal*I sites of pUJ106, resulting in constructs pUJ109, pUJ110 and pUJ111. This creates translational fusions between the different *fliF* alleles and the truncated *fliG* gene, with a short intermediate linker fragment coding for 13 amino acids. The three plasmids pUJ109–pUJ111 were then introduced into the chromosome of LS1218 by homologous recombination, yielding strains LS1992, LS1993 and LS1994.

Immunoblots

Immunoblots were performed as described by Harlow and Lane (1988) using polyclonal serum that specifically recognizes the FliF or FliM protein (Jenal *et al.*, 1994). Total protein extracts were separated by electrophoresis on 10% polyacrylamide gels and transferred overnight (4°C, 20 mA) to an Immobilon-P membrane. Primary antibody was diluted 1:5000 before use, and the secondary antibody (goat anti-rabbit IgG, HRP-coupled) was used in a 1:10 000 dilution. To reduce background, the secondary antibody was preadsorbed to NA1000 acetone powders for 1 h, as described (Harlow and Lane, 1988). Immunoblots were developed using the Renaissance kit from DuPont NEN, following the manufacturer's instructions.

Cell cycle experiments

Caulobacter crescentus wild-type and mutant cells were synchronized as described previously (Stephens and Shapiro, 1993). Isolated swarmer cells were released into fresh minimal medium at 30°C at an A_{660} of 0.3–0.4. At 20 min intervals, samples were removed for immunoblot analysis. For the determination of FliF expression during the cell cycle, 1 ml samples were removed at 20 min intervals and pulse labelled for 5 min with 5–10 μCi [^{35}S]methionine (Trans-label, ICN). Cells were then collected by centrifugation and frozen in liquid nitrogen. Cells were lysed for 30 min on ice in 0.5 ml wash buffer (450 mM NaCl, 0.5% Triton-X100, 50 mM Tris, pH 8.3) containing 4 mg/ml lysozyme. The samples were precipitated unspecifically with 25 μl Precipitin (Gibco BRL). Equivalent counts of radiolabelled protein were then used for immunoprecipitation with anti-FliF antibody (Jenal *et al.*, 1994). Quantification was performed using a Molecular Dynamics PhosphorImager with ImageQuant software.

Synchronized cultures were also allowed to proceed through the cell cycle and then harvested immediately after cell division. Swarmer and stalked cell progenies were separated by ludox density gradient centrifugation. For pulse–chase experiments, cells were labelled during the predivisional stage for 5 min with 5 μCi/ml [^{35}S]methionine (Trans-label, ICN) and chased until cell division was completed. Samples of pure swarmer and stalked cells were then used for immunoprecipitation with the anti-FliF antibody.

FliF topology studies

FliF protein fusions to β-galactosidase and β-lactamase were generated at the *fliF* internal *Pst*I and *Bgl*II sites, and at the *Sal*I site at the *fliF* 3′ end. *Bam*HI–*Pst*I, *Bam*HI–*Bgl*II and *Bam*HI–*Sal*I fragments containing different *fliF* fragments and the *fliF* promoter region were cloned into the fusion vectors pJBZ280, pJBZ281, pJAMY30 and pJAMY31. Fusion at the *Pst*I site resulted in plasmids p1P1 (β-galactosidase) and pUJ114 (β-lactamase), fusions at the *Bgl*II site resulted in plasmids p1B1 (β-galactosidase) and pUJ49 (β-lactamase), and fusions at the *Sal*I site resulted in plasmids p0S5 (β-galactosidase) and pUJ73 (β-lactamase).

Plasmids p1P1, p1B1 and p0S5 were introduced into the chromosome of wild-type strain NA1000 (strains LS785–LS787); plasmids pUJ49, pUJ73 and pUJ114 were introduced into the chromosome of strain LS107 (LS1535, LS1702, LS2252). β-Galactosidase units in strains LS785–LS787 were determined as described by Miller (1972); the minimal inhibitory concentration of ampicillin for strains LS1535, LS1702 and LS2252 was determined by detecting growth in liquid media containing different concentrations of ampicillin.

Determination of the stability of FliF derivatives

Cultures of the *fliF* null strain LS1218 carrying plasmids pUJ101 (Δ3), pUJ102 (Δ4), pUJ103 (Δ5) and pUJ104 (wt *fliF*) were pulse labelled with 5 μCi/ml [^{35}S]methionine (Trans-label, ICN) for 5 min and chased for different time periods. Cells were collected by centrifugation and frozen immediately in liquid nitrogen. The amount of labelled FliF protein present was determined by immunoprecipitation with an anti-FliF antibody, as described above. Precipitated FliF protein was analysed on 10% SDS–polyacrylamide gels and quantitated on a Molecular Dynamics PhosphorImager using ImageQuant software.

Motility assays and microscopy

The motility of *C.crescentus* wild-type and mutant strains was analysed microscopically and by stabbing cultures onto the surface of semisolid agar plates containing 0.3% agar.

Electron microscopy of whole cells was performed on a Philips 301 electron microscope at 60 kV with carbon-coated copper grids. Preparation of the grids and staining of the cells with 1% uranyl acetate was performed as described previously (Wright and Rine, 1989). Cells were harvested at different culture densities, and 10–100 μl of the cell culture was placed directly onto a grid. Grids were then washed several times with distilled water, stained and air dried before viewing.

Acknowledgements

We thank A.Newton for the plasmid pGIR230; Dickon Alley, Chris Mohr, Kim Quon and Rick Roberts for plasmids and vectors; and members of the Shapiro laboratory for helpful discussions, suggestions and critical reading of the manuscript. This work was supported by National Institutes of Health grant GM32506/512OMZ. U.J. was supported by grant 823A-040130 from the Swiss National Science Foundation.

References

Alley,M.R., Maddock,J.R. and Shapiro,L. (1992) Polar localization of a bacterial chemoreceptor. *Genes Dev.*, **6**, 825–836.

Alley,M.R.K., Maddock,J.R. and Shapiro,L. (1993) Requirement of the carboxyl terminus of the bacterial chemoreceptor for its targeted proteolysis. *Science*, **259**, 1754–1757.

Brun,Y.V., Marczynski,G. and Shapiro,L. (1994) The expression of asymmetry during *Caulobacter* cell differentiation. *Annu. Rev. Biochem.*, **63**, 419–450.

Champer,R., Dingwall,A. and Shapiro,L. (1987) Cascade regulation of *Caulobacter* flagellar and chemotaxis genes. *J. Mol. Biol.*, **194**, 71–80.

Driks,A., Bryan,R., Shapiro,L. and DeRosier,D.J. (1989) The organization of the *Caulobacter crescentus* flagellar filament. *J. Mol. Biol.*, **206**, 627–636.

Ely,B. (1991) Genetics of *Caulobacter crescentus*. *Methods Enzymol.*, **204**, 372–384.

Evinger,M. and Agabian,N. (1977) Envelope-associated nucleoid from *Caulobacter crescentus* stalked and swarmer cells. *J. Bacteriol.*, **132**, 294–301.

Francis,N.R., Irikura,V.M., Yamaguchi,S., DeRosier,D.J. and Macnab, R.M. (1992) Localization of the *Salmonella typhimurium* flagellar switch protein FliG to the cytoplasmic M-ring face of the basal body. *Proc. Natl Acad. Sci. USA*, **89**, 6304–6308.

Francis,N.R., Sosinsky,G.E., Thomas,D. and DeRosier,D.J. (1994) Isolation, characterization and structure of bacterial flagellar motors containing the switch complex. *J. Mol. Biol.*, **235**, 1261–1270.

Gamer,J., Bujard,H. and Bukau,B. (1992) Physical interaction between heat shock proteins DnaK, DnaJ, and GrpE and the bacterial heat shock transcription factor sigma 32. *Cell*, **69**, 833–842.

Ghoda,L., van Daalen Wetters,T., Macrae,M., Ascherman,D. and Coffino,P. (1989) Prevention of rapid intracellular degradation of ODC by a carboxyl-terminal truncation. *Science*, **243**, 1493–1495.

Ghoda,L., Phillips,M.A., Bass,K.E., Wang,C.C. and Coffino,P. (1990) Trypanosome ornithine decarboxylase is stable because it lacks sequences found in the carboxyl terminus of the mouse enzyme which target the latter for intracellular degradation. *J. Biol. Chem.*, **265**, 11823–11826.

Ghoda,L., Sidney,D., Macrae,M. and Coffino,P. (1992) Structural elements of ornithine decarboxylase required for intracellular degradation and polyamine-dependent regulation. *Mol. Cell Biol.*, **12**, 2178–2185.

Glotzer,M., Murray,A.W. and Kirschner,M.W. (1991) Cyclin is degraded by the ubiquitin pathway. *Nature*, **349**, 132–138.

Gober,J.W. and Marques,M.V. (1995) Regulation of cellular differentiation in *Caulobacter crescentus*. *Microbiol. Rev.*, **59**, 31–47.

Gober,J.W., Champer,R., Reuter,S. and Shapiro,L. (1991) Expression of positional information during cell differentiation of *Caulobacter*. *Cell*, **64**, 381–391.

Hara,H., Yamamoto,Y., Higashitani,A., Suzuki,H. and Nishimura,Y. (1991) Cloning, mapping, and characterization of the *Escherichia coli prc* gene, which is involved in C-terminal processing of penicillin-binding protein 3. *J. Bacteriol.*, **173**, 4799–4813.

Harlow,E. and Lane,D. (1988) *Antibodies: A Laboratory Manual*. Cold Spring Harbor Laboratory Press, Cold Spring Harbor, NY, pp. 479–510.

Herman,C., Thevenet,D., D'Ari,R. and Bouloc,P. (1995) Degradation of sigma 32, the heat shock regulator in *Escherichia coli*, is governed by HflB. *Proc. Natl Acad. Sci. USA*, **92**, 3516–3520.

Homma,M., Aizawa,S., Dean,G.E. and Macnab,R.M. (1987) Identification of the M-ring protein of the flagellar motor of *Salmonella typhimurium*. *Proc. Natl Acad. Sci. USA*, **84**, 7483–7487.

Horii,T., Ogawa,T., Nakatani,T., Hase,T., Matsubara,H. and Ogawa,H. (1981) Regulation of SOS functions: purification of *E. coli* LexA protein and determination of its specific site cleaved by the RecA protein. *Cell*, **27**, 515–522.

Hynes,M.F., Quandt,J., O'Connell,M.P. and Puehler,A. (1989) Direct selection for curing and deletion of *Rhizobium* plasmids using transposons carrying the *Bacillus subtilis sacB* gene. *Gene*, **78**, 111–120.

Jenal,U., White,J. and Shapiro,L. (1994) *Caulobacter* flagellar function, but not assembly, requires FliL, a non-polarly localized membrane protein present in all cell types. *J. Mol. Biol.*, **243**, 227–244.

Jones,C.J. and Macnab,R.M. (1990) Flagellar assembly in *Salmonella typhimurium*: analysis with temperature-sensitive mutants. *J. Bacteriol.*, **172**, 1327–1339.

Jones,C.J., Homma,M. and Macnab,R.M. (1989) L-, P-, and M-ring proteins of the flagellar basal body of *Salmonella typhimurium*:

gene sequences and deduced protein sequences. *J. Bacteriol.*, **171**, 3890–3900.

Jones,C.J., Macnab,R.M., Okino,H. and Aizawa,S. (1990) Stoichiometric analysis of the flagellar hook–basal–body complex of *Salmonella typhimurium*. *J. Mol. Biol.*, **212**, 377–387.

Kang,P.J. and Shapiro,L. (1994) Cell cycle arrest of a *Caulobacter crescentus secA* mutant. *J. Bacteriol.*, **176**, 4958–4965.

King,R.W., Jackson,P.K. and Kirschner,M.W. (1994) Mitosis in transition. *Cell*, **79**, 563–571.

Kubori,T., Shimamoto,N., Yamaguchi,S., Namba,K. and Aizawa,S.-I. (1992) Morphological pathway of flagellar assembly in *Salmonella typhimurium*. *J. Mol. Biol.*, **226**, 433–446.

Larsen,S.H., Adler,J., Gargus,J.J. and Hogg,R.W. (1974) Chemomechanical coupling without ATP: the source of energy for motility and chemotaxis in bacteria. *Proc. Natl Acad. Sci. USA*, **71**, 1239–1243.

Liberek,K. and Georgopoulos,C. (1993) Autoregulation of the *Escherichia coli* heat shock response by the DnaK and DnaJ heat shock proteins. *Proc. Natl Acad. Sci. USA*, **90**, 11019–11023.

Liberek,K., Galitski,T.P., Zylicz,M. and Georgopoulos,C. (1992) The DnaK chaperone modulates the heat shock response of *Escherichia coli* by binding to the sigma 32 transcription factor. *Proc. Natl Acad. Sci. USA*, **89**, 3516–3520.

Liberek,K., Wall,D. and Georgopoulos,C. (1995) The DnaJ chaperone catalytically activates the DnaK chaperone to preferentially bind the sigma 32 heat shock transcriptional regulator. *Proc. Natl Acad. Sci. USA*, **92**, 6224–6228.

Little,J.W., Edmiston,S.H., Pacelli,L.Z. and Mount,D.W. (1980) Cleavage of the *Escherichia coli* LexA protein by the RecA protease. *Proc. Natl Acad. Sci. USA*, **77**, 3225–3229.

Loetscher,P., Pratt,G. and Rechsteiner,M. (1991) The C-terminus of mouse ornithine decarboxylase confers rapid degradation on dihydrofolate reductase. Support for the PEST hypothesis. *J. Biol. Chem.*, **266**, 11213–11220.

Macnab,R.M. (1992) Genetics and biogenesis of bacterial flagella. *Annu. Rev. Genet.*, **26**, 131–158.

Manoil,C. (1990) Analysis of protein localization by use of gene fusions with complementary properties. *J. Bacteriol.*, **172**, 1035–1042.

Manoil,C., Boyd,D. and Beckwith,J. (1988) Molecular genetic analysis of membrane protein topology. *Trends Genet.*, **4**, 223–226.

Manson,M.D., Tedesco,P., Berg,H.C., Harold,F.M. and Van der Drift,C. (1977) A protonmotive force drives bacterial flagella. *Proc. Natl Acad. Sci. USA*, **74**, 3060–3064.

Miller,J.H. (1972) *Experiments in Molecular Genetics*. Cold Spring Harbor Laboratory Press, Cold Spring Harbor, NY, pp. 352–355.

Nagai,H., Yuzawa,H., Kanemori,M. and Yura,T. (1994) A distinct segment of the sigma 32 polypeptide is involved in DnaK-mediated negative control of the heat shock response in *Escherichia coli*. *Proc. Natl Acad. Sci. USA*, **91**, 10280–10284.

Newton,A., Ohta,N., Ramakrishnan,G., Mullin,D. and Raymond,G. (1989) Genetic switching in the flagellar gene hierarchy of *Caulobacter* requires negative as well as positive regulation of transcription. *Proc. Natl Acad. Sci. USA*, **86**, 6651–6655.

Ohta,N., Chen,L.S., Mullin,D.A. and Newton,A. (1991) Timing of flagellar gene expression in the *Caulobacter* cell cycle is determined by a transcriptional cascade of positive regulatory genes. *J. Bacteriol.*, **173**, 1514–1522.

Okino,H., Isomura,M., Yamaguchi,S., Magariyama,Y., Kudo,S. and Aizawa,S.I. (1989) Release of flagellar filament–hook–rod complex by a *Salmonella typhimurium* mutant defective in the M ring of the basal body. *J. Bacteriol.*, **171**, 2075–2082.

Oosawa,K., Ueno,T. and Aizawa,S. (1994) Overproduction of the bacterial flagellar switch proteins and their interactions with the MS-ring complex *in vitro*. *J. Bacteriol.*, **176**, 3683–3691.

Parsell,D.A., Silber,K.R. and Sauer,R.T. (1990) Carboxy-terminal determinants of intracellular protein degradation. *Genes Dev.*, **4**, 277–286.

Prinz,W.A. and Beckwith,J. (1994) Gene fusion analysis of membrane protein topology: a direct comparison of alkaline phosphatase and β-lactamase fusions. *J. Bacteriol.*, **176**, 6410–6413.

Pugsley,A.P. (1993) The complete general secretory pathway in Gram-negative bacteria. *Microbiol. Rev.*, **57**, 50–108.

Quon,K.C., Marczynski,G.T. and Shapiro,L. (1996) An essential bacterial two-component signal transduction protein controls multiple cell cycle events in *Caulobacter*. *Cell*, **84**, 1–20.

Ramakrishnan,G., Zhao,J.L. and Newton,A. (1994) Multiple structural proteins are required for both transcriptional activation and negative autoregulation of *Caulobacter crescentus* flagellar genes. *J. Bacteriol.*, **176**, 7587–7600.

Sambrook,J., Fritsch,E.F. and Maniatis,T. (1989) *Molecular Cloning. A Laboratory Manual*. Cold Spring Harbor Laboratory Press, Cold Spring Harbor, NY, pp. A1–A13.

Shapiro,L. (1995) The bacterial flagellum: from genetic network to complex architecture. *Cell*, **80**, 525–527.

Shapiro,L. and Maizel,J. (1973) Synthesis and structure of *Caulobacter crescentus* flagella. *J. Bacteriol.*, **113**, 478–485.

Silber,K.R., Keiler,K.C. and Sauer,R.T. (1992) Tsp: a tail-specific protease that selectively degrades proteins with nonpolar C-termini. *Proc. Natl Acad. Sci. USA*, **89**, 295–299.

Silverman,M. and Simon,M. (1974) Flagellar rotation and the mechanism of bacterial motility. *Nature*, **249**, 73–74.

Simon,R., Prieffer,U. and Puhler,A. (1983) A broad host range mobilization system for *in vivo* genetic engineering: transposon mutagenesis in Gram negative bacteria. *Biotechnology*, **1**, 784–790.

Sosinsky,G.E., Francis,N.R., DeRosier,D.J., Wall,J.S., Simon,M.N. and Hainfeld,J. (1992) Mass determination and estimation of subunit stoichiometry of the bacterial hook–basal body flagellar complex of *Salmonella typhimurium* by scanning transmission electron microscopy. *Proc. Natl Acad. Sci. USA*, **89**, 4801–4805.

Stallmeyer,M.J., Hahnenberger,K., Sosinsky,G.E., Shapiro,L. and DeRosier,D. (1989a) Image reconstruction of the flagellar basal body of *Caulobacter crescentus*. *J. Mol. Biol.*, **205**, 511–518.

Stallmeyer,M.J., Aizawa,S., Macnab,R.M. and DeRosier,D.J. (1989b) Image reconstruction of the flagellar basal body of *Salmonella typhimurium*. *J. Mol. Biol.*, **205**, 519–528.

Stephens,C.M. and Shapiro,L. (1993) An unusual promoter controls cell-cycle regulation and dependence on DNA replication of the *Caulobacter fliLM* early flagellar operon. *Mol. Microbiol.*, **9**, 1169–1179.

Stephens,C.M., Zweiger,G. and Shapiro,L. (1995) Coordinate cell cycle control of a *Caulobacter* DNA methyltransferase and the flagellar genetic hierarchy. *J. Bacteriol.*, **177**, 1662–1669.

Straus,D., Walter,W. and Gross,C.A. (1990) DnaK, DnaJ, and GrpE heat shock proteins negatively regulate heat shock gene expression by controlling the synthesis and stability of sigma 32. *Genes Dev.*, **4**, 2202–2209.

Tilly,K., Spence,J. and Georgopoulos,C. (1989) Modulation of stability of the *Escherichia coli* heat shock regulatory factor sigma. *J. Bacteriol.*, **171**, 1585–1589.

Tomoyasu,T. *et al.* (1995) *Escherichia coli* FtsH is a membrane-bound, ATP-dependent protease which degrades the heat-shock transcription factor sigma 32. *EMBO J.*, **14**, 2551–2560.

Trachtenberg,S. and DeRosier,D.J. (1992) A three-start helical sheath on the flagellar filament of *Caulobacter crescentus*. *J. Bacteriol.*, **174**, 6198–6206.

Ueno,T., Oosawa,K. and Aizawa,S. (1992) M-ring, S-ring and proximal rod of the flagellar basal body of *Salmonella typhimurium* are composed of subunits of a single protein, FliF. *J. Mol. Biol.*, **227**, 672–677.

Ueno,T., Oosawa,K. and Aizawa,S. (1994) Domain structures of the MS-ring component protein (FliF) of the flagellar basal body of *Salmonella typhimurium*. *J. Mol. Biol.*, **236**, 546–555.

Wingrove,J.A. and Gober,J.W. (1994) A sigma 54 transcriptional activator also functions as a pole-specific repressor in *Caulobacter*. *Genes Dev.*, **8**, 1839–1852.

Wingrove,J.A., Mangan,E.K. and Gober,J.W. (1993) Spatial and temporal phosphorylation of a transcriptional activator regulates pole-specific gene expression in *Caulobacter*. *Genes Dev.*, **7**, 1979–1992.

Wright,R. and Rine,J. (1989) Transmission electron microscopy and immunocytochemical studies of yeast: analysis of HMG-CoA reductase overproduction by electron microscopy. *Methods Cell Biol.*, **31**, 473–512.

Yu,J. and Shapiro,L. (1992) Early *Caulobacter crescentus* genes *fliL* and *fliM* are required for flagellar gene expression and normal cell division. *J. Bacteriol.*, **174**, 3327–3338.

Zhao,R., Schuster,S.C. and Khan,S. (1995) Structural effects of mutations in *Salmonella typhimurium* flagellar switch complex. *J. Mol. Biol.*, **251**, 400–412.

Zhuang,W.Y. and Shapiro,L. (1995) *Caulobacter* FliQ and FliR membrane proteins, required for flagellar biogenesis and cell division, belong to a family of virulence factor export proteins. *J. Bacteriol.*, **177**, 343–356.

Received on November 8, 1995; revised on January 23, 1996